School of Physics

Trinity College Dublin
The University of Dublin

The Fast Transient Sky

Stage Transfer Report

Owen Johnson[†]
Astrophysics Group
February, 2024

Abstract

The abstract is a short concise outline of your project area, **of no more than 100 words**.

Supervisor: Assoc. Prof. Evan Keane

[†]ojohnson@tcd.ie

Contents

1 A Prelude to Pulsars **1**

1.1 The Population of Pulsars 1

1.2 The Properities of Pulsars 2

1.2.1 Neutron Star Radius & Mass 3

1.2.2 Spin Evolution 3

1.2.3 Braking Index 4

1.2.4 Dispersion Measure 5

1.3 Pulsar Subclasses 6

1.4 Spider Pulsars 6

1.5 Why study Redback Pulsars? 8

1.6 Other exotic transients 8

1.6.1 Dwarf Stars 8

1.6.2 SETI 8

2 Work This Far / Method and Results **9**

2.1 Observation Campaigns 9

2.2 Observation Data 10

2.3 Search Strategy 10

2.3.1 RFI Removal 11

2.3.2 Incoherent Dedispersion 11

2.3.3 Fast Fourier Transform 12

2.3.4 Accelration Searching 13

3 Summary **15**

Declaration

I hereby declare that this report is entirely my own work and that it has not been submitted as an exercise for a degree at this or any other university.

I have read and I understand the plagiarism provisions in the General Regulations of the University Calendar for the current year, found at http://www.tcd.ie/calendar.

Signed: _____ Date: _____

Publications and Presentations

Publications

Johnson, O.A., Gajjar, V., Keane, E.F., et. al (2023). Simultaneous dual-site SETI with LOFAR international stations. Manuscript accepted for publication to AJ. arXiv:2310.15704

Presentations

1. Low Frequency's Place in SETI, January, 2024, PSETI Symposium, Penn State. [**Invited**]
2. Technosignatures with NenuFAR, December, 2023, Science at Low Frequencies IX, UvA.
3. SETI Science at 30 - 190 MHz, November, 2023, BLUK Workshop, SKAO. [**Invited**]
4. Technosignature Science at Low Frequencies, November, 2023, NASA Goddard Flight Center. [**Invited**]
5. Dual Site SETI Searches, 2023, International Astronautical Congress, Baku.

Physical Constants

Constant	Symbol	Value
Speed of Light	c	2.99792458×10^{8} m/s
Gravitational Constant	G	6.674×10^{-11} m^3 kg^{-1} s^{-2}
Planck's Constant	h	6.626×10^{-34} m^2 kg s^{-1}
Boltzmann Constant	k_B	1.381×10^{-23} m^2 kg s^{-2} K^{-1}
Stefan-Boltzmann Constant	σ	5.670×10^{-8} W m^{-2} K^{-4}
Electron Charge	e	1.602×10^{-19} C
Electron Mass	m_e	9.109×10^{-31} kg
Proton Mass	m_p	1.672×10^{-27} kg
Neutron Mass	m_n	1.675×10^{-27} kg
Solar Mass	$M_\odot$	1.989×10^{30} kg
Solar Radius	$R_\odot$	6.957×10^{8} m
Solar Luminosity	$L_\odot$	3.828×10^{26} W
Solar Temperature	$T_\odot$	5772 K
Jansky	Jy	10^{-26} W m^{-2} Hz^{-1}

1 A Prelude to Pulsars

When stars with a mass of at least $8\,M_\odot$ reach the end of their evolutionary stage they experience a depletion of nuclear fuel will and undergo a core collapse. This results in the star exploding as a Supernova. Depending on the mass of the host star the Supernova will form a black Hole or a neutron Star. Based on the electron degeneracy pressure limit (Chandrasekhar, 1967, pp. 434 - 443) stars that fall in the range of 20 - 30 $M_\odot$ form neutron stars (Heger et al., 2003).

Neutron stars are supported against further collapse by the presence of neutron degeneracy pressure which arises from the Pauli exclusion principle. Strong Nuclear forces between the neutrons also provides additional support against gravatational collapse. With these two opposing forces a stable equilibrium is formed.

In turn, this makes neutron stars exceptionally dense, they are the densest known objects in the universe that emit light. The average density of a neutron star is 10^{17}kg/m^3 (Baym et al., 1971) and their radii are comparable to the size of cities, with radii of 10 - 20 km.

During collapse the conservation of magnetic flux plays a crucial role in the large strength magnetic fields that are observed in neutron stars along with contributions from the dynamo effect and frozen-in magnetic fields. The strength of a pulsar's magnetic field is on the order of 10^{12} - 10^{15} Gauss (Michel, 1982).

Charged particles accelerate along the magnetic field lines in the magnetosphere of the neutron star. These particles emit electromagnetic radiation in a cone shape along the magnetic axis. If the magnetic axis is not aligned with the rotational axis of the neutron star, the radiation beam will sweep across the sky. This is known as a pulsar, a Galacic lighthouse.

1.1 The Population of Pulsars

At the time of writing there are currently more than 3380 known pulsars. Since their discovery by Jocelyn Bell Burnell (Hewish et al., 1968) the population has grown immensly but there remains many open questions about pulsar evolution and the subclasses that lie within the population as a whole. Similarly to how exoplanet popilations are shown using the mass-radius diagram and stellar populations are shown using the Hertzsprung-Russell diagram, pulsar populations are shown using what is known as the $P-\dot{P}$ diagram.

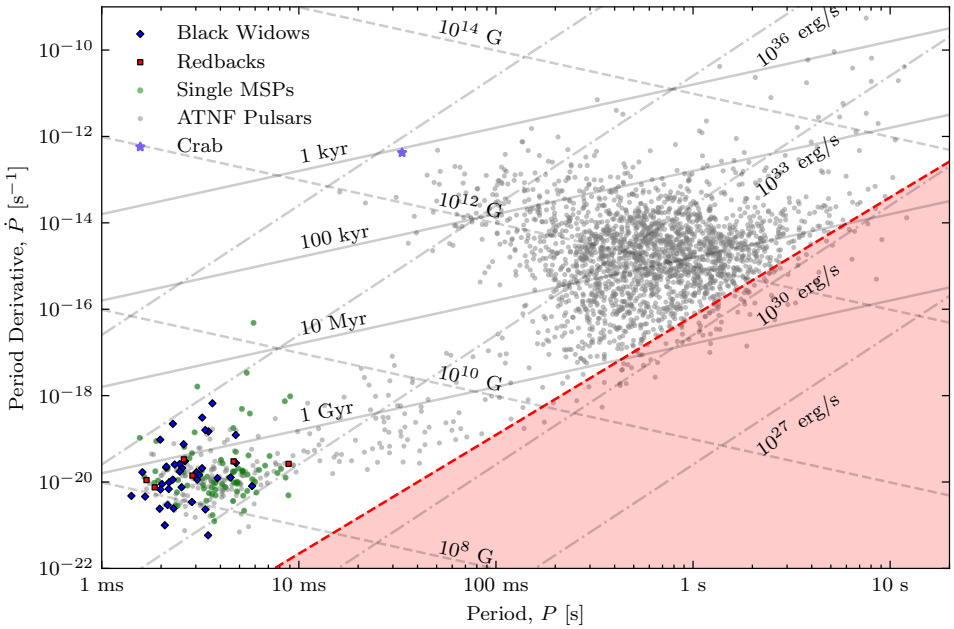

Figure 1.1: The $P - \dot{P}$ diagram showing the population of pulsars. The the milisecond pulsar subclasses are colour coded. The red region represents the death line, where pulsars are theortically no longer able to emit radio waves.

P representing the Pulsar's rotational period and $\dot{P}$ it's derivative. These are key ways that pulsars are classified and study in context of their evolution. An example of a $P - \dot{P}$ diagram is shown in fig. 1.1. Different values on the plot indicate the roughly the Pulsars age and magnetic field strength. Figure 1.1 shows the vastly different values bettween pulsars in the milisecond range and pulsars in the second range.

Theoretically it has been shown that pulsars exhibit a death line in the $P - \dot{P}$ diagram. This is the line where pulsars are no longer able to emit radio waves. This is due to the pulsar's magnetic field is no longer strong enough to accelerate particles along the magnetic field lines. However it has been shown that pulsars do exist below this line. The area below this line is commonly referred to as the "graveyard".

1.2 The Properities of Pulsars

The following section gives a breif non-exhaustive overview of some of the key properities of pulsars.

1.2.1 Neutron Star Radius & Mass

Understanding the mass of pulsars are important for understanding their evolution and equation of state. Oppenheimer and Volkoff (1939) derived a canonical mass limit of neutron stars to be 1.4 $M_\odot$, but expermientally this has been shown to be higher with the largest mass of a pulsar being $\sim 2.35\,M_\odot$ (Romani et al., 2022). The mass-radius relationship of a pulsar is defined by an equation of state and a maximum mass limit. Redshifts and gravatational effects observed in pulsars exhbit the observed temperture and flux to be smaller than the actual value. The observed radius R_{obs} can be described as follows (Lorimer and Kramer, 2004),

$$R_{\text{obs}} = \frac{R}{\sqrt{1-\frac{2GM}{Rc^2}}} = \frac{1}{R}\sqrt{1-\frac{R_s}{R}} \tag{1.1}$$

where R is the pulsar's radius and M is the gravatational mass, G is the gravatational constant, c is the speed of light and R_s is the Schwarzschild radius.
The lower limit of the neutron star radius is decribed by

$$R_{\text{min}} \simeq 1.5\ R_s = \frac{3GM}{c^2} = 6.2\ \text{km}\left(\frac{M}{1.4\,M_\odot}\right) \tag{1.2}$$

Opposite to this upper limit of the radius is obtained by requiring that there is stability against breaking up due to centrifulgal forces. This gives eq. (1.3) following as described in (Lorimer and Kramer, 2004, p. 58).

$$R_{\text{max}} \simeq \left(\frac{GMP^2}{4\pi^2}\right)^{1/3} = 16.8\ \text{km}\left(\frac{M}{1.4\,M_\odot}\right)^{1/3}\left(\frac{P}{\text{ms}}\right)^{2/3} \tag{1.3}$$

Most pulsars are observed to have radii in the range of 10 - 15 km (Lattimer and Prakash, 2001), giving them the unique position of 'almost' black holes.

1.2.2 Spin Evolution

One of the most unique characterstics of pulsars is the spinning that they exhibit. Understanding the spin evolution gives insight into many parameters of the pulsars most notable the stage of their evolution. Pulsar's begin their life in the upper end of the $P-\dot{P}$ diagram and slowly move down and to the right as they age due to a loss in rotational energy, commonly referred to as spin-down luminosity. The spin-down ($\dot{E}$) is decribed as follows (Lorimer and Kramer, 2004, p. 59),

$$\dot{E} = -\frac{dE_{\text{rot}}}{dt} = 4\pi^2 I \dot{P} P^{-3} \tag{1.4}$$

Where I is the moment of inertia. It is important to note that the energy loss that is converted into radio emmision is almost negligable in comparison to the total energy loss from spin down.

1.2.3 Braking Index

Pulsar's have strong magnetic dipoles, according to classic mechanics a rotating magnetic doplole that exhibts a moment, $|m|$ emits an electromagnetic wave at the pulsars rotation frequency (Lorimer and Kramer, 2004, p. 60). The dipoles radiation power is characterized by,

$$\dot{E}_{\text{dipole}} = \frac{2}{3c^3}|m|^2\omega^4 \sin^2\alpha \tag{1.5}$$

Where α is the angle between the magnetic axis and the rotation axis. Equating the above equation to the loss of rotational energy described in eq. (1.4) gives the following for the expected evolution of the period,

$$\dot{\Omega} = -\frac{2}{3Ic^3}|m|^2\Omega^3 \sin^2\alpha \tag{1.6}$$

This is more commonly written ass a power law,

$$\dot{\nu} = -K\nu^n \tag{1.7}$$

Equation (1.4) in terms of the period is, $\dot{P} = KP^{2-n}$. Since this is a first order differential equation, the solution can be intergrated and given a constant, K which provides and expression of age.

$$T = \frac{P}{(n-1)\dot{P}}\left\{1 - \left(\frac{P_0}{P}\right)^{n-1}\right\} \tag{1.8}$$

Here P_0 is the initial period of the pulsar. Commomly an assumption is made that the current perios is much greater than the intial period ($P_0 \ll P$). If it is also assumped that the pulsar is spinning down to due dipole magnetic radiaiton ($n = 3$), eq. (1.8) can be simplified into a charaactertic age.

$$\tau_c \cong 15.8 \text{ Myr} \left(\frac{P}{s}\right) \left(\frac{\dot{P}}{10^{-15}}\right)^{-1} \tag{1.9}$$

The above estimation for a pulsars age is known to be inconsistent with theorey to varying degrees. In cases where a Supernovae has been observed and produced a pulsar the age is known to a much higher degree of accuracy. The Crab pulsar is one such example with an observed Supernova event in 1054 AD by Chinese astronmers (Kaspi et al., 2001).

1.2.4 Dispersion Measure

The interstellar medium (ISM) is a complex mixture of gas, dust and magnetic fields that fills the space between stars in a galaxy. Given that the ISM is a cold and ionised plasma any electromagnetic radiation will undergo a frequency-depedant index of refraction as they propagate. The following equation describes the refractive index of the ISM neglciting Galactic magnetic field (Lorimer and Kramer, 2004, p. 85),

$$\mu = \sqrt{1 - \left(\frac{f_p}{f}\right)^2} \tag{1.10}$$

Where f_p is the plasma frequency, $8.5 \text{ kHz} \, (n_e/\text{cm}^{-3})^{1/2}$ and f is the frequency of the observed radiation.
If the refractive index of the ISM $\mu < 1$ then it can be assumed that the group velocity of the radiation is $v_g = c\mu$ which is sub light speed. The path of radiotion from a pulsar to the observer will be delayed in time with respect to a infinite frequecy by an amount,

$$t = \left(\int_0^d \frac{dl}{v_g}\right) - \frac{d}{c} \tag{1.11}$$

If is assmumed to be $f_p \ll f$, μ can be approximated.

$$t = \frac{1}{c}\int_0^d \left(1 + \frac{f_p^2}{2f^2}\right) dl - \frac{d}{c} = \frac{e^2}{2\pi m_e c} \frac{\int_0^d n_e \, dl}{f^2} \equiv \mathcal{D} \cdot \frac{\text{DM}}{f^2} \tag{1.12}$$

Where $\mathcal{D}$ is the dispersion constant and DM is the dispersion measure. Each are commonly expressed as follows, $\mathcal{D} = 4.15 \times 10^3 \text{ MHz}^2 \text{ pc}^{-1} \text{ cm}^3 \text{ s}$ and $\text{DM} = \int_0^d n_e \, dl \text{ cm}^{-3} \text{ pc}$. This definition was adapted from Lorimer and Kramer (2004, p. 86) and Taylor and Manchester (1977).

1.3 Pulsar Subclasses

Following breif overview of the properities of pulsars, this section will give a breif overview of the subclasses of pulsars. The population of pulsars can be broken down into subclasses based on unique patterns in their properities. The main subclasses[1] are as follows:

1. Normal Pulsars: These are the most common type of pulsars. They are characterized by their regular pulses and are often observed in radio wavelengths. They are also known as radio pulsars.

2. Rotating Radio Transients (RRATs): These are a subclass of pulsars that were initially discovered through their sporadic radio bursts rather than regular pulses. They exhibit irregular and infrequent radio emission.

3. Magnetars: While not exclusively pulsars, magnetars are highly-magnetized neutron stars that can also emit pulsed radiation. They are characterized by extremely strong magnetic fields, much more intense than typical pulsars.

4. Binary Pulsars: These are pulsars that are in orbit around another star, usually a normal (non-neutron) star. The interaction with the companion star can have significant effects on the pulsar's behavior.

5. Millisecond Pulsars (MSPs): These are pulsars with very short rotation periods, typically less than 10 milliseconds. They are believed to be old pulsars that have been spun up by the accretion of mass from a companion star in a binary system.

6. X-ray Pulsars: Pulsars that emit pulsed X-ray radiation fall into this category. These pulsars are typically observed in binary systems where the pulsar accretes matter from its companion star, leading to X-ray emission.

7. Anomalous X-ray Pulsars (AXPs) and Soft Gamma-ray Repeaters (SGRs): These are closely related to magnetars and are characterized by their intense and variable X-ray and gamma-ray emission. They are believed to be neutron stars with extremely strong magnetic fields.

1.4 Spider Pulsars

The type of pulsar that is of interest to this project is a subclass of transional miliscond pulsars known as Spider Pulsars. Spider pulsars fall into two categories depending on their orbiting companion. The first category are known as Black Widow pulsars segreated based on their companion mass falling in the range of 0.01 - 0.05 $M_\odot$ with a compantion

[1] This is a non-exhaustive list.

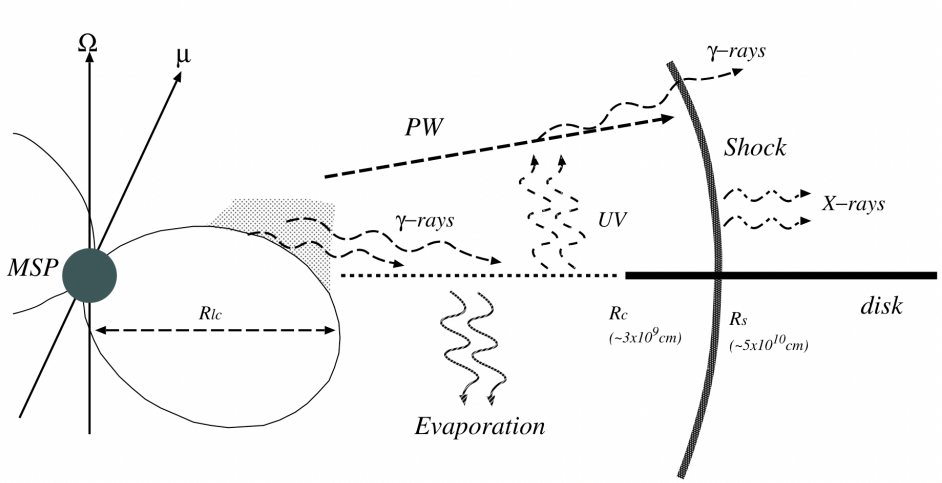

Figure 1.2: Figure taken from Takata et al. (2014). Example of multiwavelength emission from a Redback pulsar.

orbital period (P_B) of less than 10 hours (citation). The second category are known as Redback pulsars and have a companion mass of 0.2 $M_\odot$ or greater with a P_B of less than 1 day (citation).

It is thought that most milisecond pulsars are formed through the accretion of matter from a evolved compact binary system, the $\sim$ 30% found in isolation are thought to have ablated their companion star to the point of dissapaction (citation). Matieral being thrown off the pulsar causes the radio emission to be eclipsed via scattering and absorption, for a segment of the companion's orbit. Rebacks systems exhibit both positive and negative period derivatives that are larger than the expected gravatiational radiation and is thought to a-rise from the interaction of the companion's magnetuc field and the pulsar's wind (citation).
Redback pulsars have been observed in two transional states ablation and accretion states (citation). These states are on sub year timescales. The transition in stages sees the magnitude of optical emission to increase by about $\sim$ 1 order of magnitude. Studying optical emission from redback pulsars informs on the heating of the companion. Roche-lobe filling fraction and the mass of the system (citation).
Black widow pulsars have been observed to have little to no observable X-ray emission (citation). However, redaback's have been shown to exhibit much more x-ray emission in their thermal spectra with consistent double peaks obseravble when the pulsar is at inferior conjunction (citation).
The observed companions of redbacks are mostly faint stars with tempertures around X on the farside of the star from the pulsar. The companion's interaction with the pulsar dominates the thermal spectrum of spider pulsars from the present heating between the two.

X-ray emission from redbacks shows hard X-ray spectra that follows a power law with photon indices (Γ) around 1 - 1.3. The energy of the thermal spectra in the X-ray is higher than what is expected from shock acceleration. Some models suggest tgat a wind-wind shock betweeb the pulsar and companion. However, this approach would require the wind momentum of the pulsar to be much weaker than the companion's. But similarly with the optical emission, the X-ray emission may be influenced by the magnetic field of the companion.

1.5 Why study Redback Pulsars?

Redback pulsars have a number of interesting science cases. Redbacks undergo a range of phenomena, including radio and X-ray pulsations, accretion processes, and periodic eclipses as the companion star passes in front of the pulsar. Their study also provides valuable insights into the evolution of binary systems, the behavior of pulsars, and the physics of accretion processes.. Due to their transitional nature they provide a glimpse into the evolution of pulsars in the latter stages of their evolution. Pulsars are also used as tools to study theories of gravity, the interstellar medium and probe for gravatational waves.

1.6 Other exotic transients

Redbacks themselves exotic transients, but there are many other clases of radio exotica that are of interest for the community. In this project work has also been carried out on an array of various radio transients and related objects. This includes the search for extraterrestrial intellgience (SETI), the study of M and Brown dwarf radio flares and the probing of potential radio emission from exoplanets.

1.6.1 Dwarf Stars

1.6.2 SETI

The search for life elsewhere in the universe as always been a burning question for many astronmers throughotu history, even more the previlance of intellgient life in the universe. Since the 1960's there has been consisent surveys, mainly in radio that look for signals of artifical origin, commonly referred to as technosignature. These signatures are thought to be similar to that of radio signals produced artifically on Earth. These signals are mainly thought to be narrowband drifiting radio emission that would be produced by a transmitter leaking into space. To date there has been no positive detection of a technosignature. Similar to dark matter searches, the lack of detections has allowed for

limits to be placed on the number of previlance of civilizations in the galaxy.

$$N = R_* \cdot f_p \cdot n_e \cdot f_l \cdot f_i \cdot f_c \cdot L \tag{1.13}$$

2 Work This Far / Method and Results

As outlined in section 1 the study of redback pulsars has a multitude of science cases. However, the number of known redback is small, in searching for new redback pulsars allows for further inquiry into the nature of the subclass. The search usually begins with the selection of potential candidates from large-scale surveys carried out by optical, X-ray and γ-ray observatories. Candiates are determined based on the flaring exhibted at these shorter wavelengths, then followed up using radio telescopes. Work to date has been to perform follow-up radio observations of Redback candidates to attempt to confirm radio emission and further compliment prior multiwavelength studies.

The *Fermi* Large Area Telescope (LAT) provides the most candidates as the related γ-ray emission are not subject to the same limitations as other detection methods (Ray et al., 2012). Both candidates observed so far as part of this project are two Fermi candidates 1FGL J0523.5-2529 and 4FGL J2054.2+6904.

2.1 Observation Campaigns

J0523 was the first observed candidate and was observed using the Ultra-Wide-Bandwidth, Low Frequency Reciver (UWL)[2] on the Parkes Murriyang telescope in New South Wales. Published studies from Strader et al. (2014) and Halpern et al. (2022) provide the orbital period, companion's radial velocity and distance measurements for the system. Each of these factors are important in determining the observation and search strategy.

For the pulsar to be detected the radio emission from the poles must be visible to the observer plane of view and the beam must be unobsured by the companion star. The orbital phase can be easily calculated from the periodic emission in the optical as demonstrated in fig. 2.1 using the following equation,

$$\phi = \frac{t - T_0}{P_{\text{orb}}} \tag{2.1}$$

At the time of writing 74% of the orbital phase has been observed, with time approved

[2]The UWL operates from 704 to 4032 MHz (40 - 7 cm)

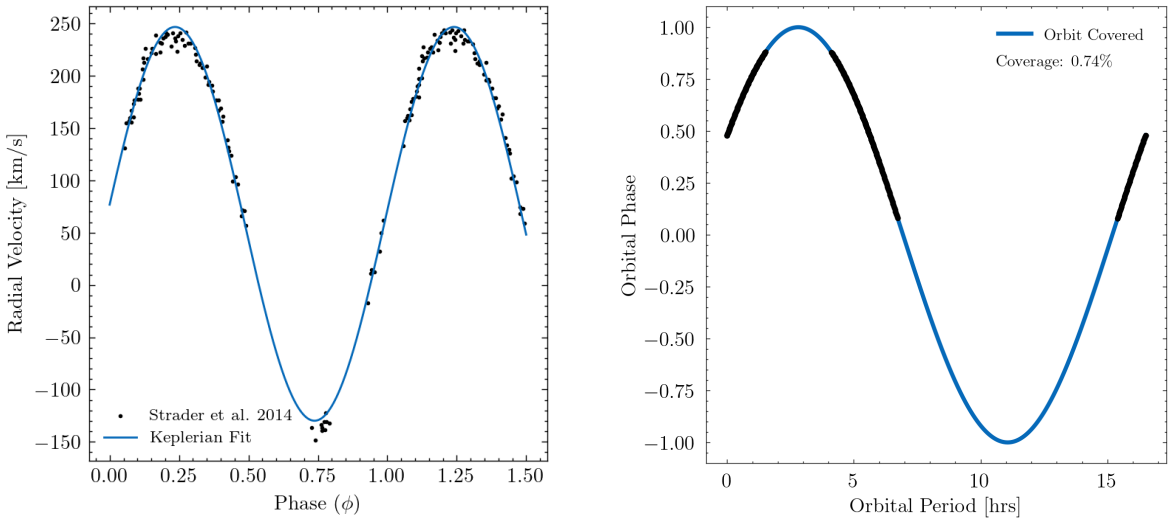

(a) Phased radial velocities observed from the optical counterpart of J0523 with the Keplerian fit overplotted

(b)

Figure 2.1

to observe the remaining orbital phase if the pulsar is not detected.

In the case of J2054 less information is known with no accurate phase ephermeris avalible. A study by Karpova et al. (2023) reports the period, companion radius and distance. Over 8 hours of observations have been carried out using I-LOFAR. In this case the entire orbit needs to be covered and blindly searched for radio emission within expected parameter range of a Redback pulsar. Observations with X are planned to take place in the Summer of 2024 to try and determine the orbital phase based.

2.2 Observation Data

Observations from radio telescopes typically includes measurements of intensity, frequency, polarization and time. The data is usually stored in a time series format with the intensity and frequency measurements recorded at each time step. The data is usually stored in a filterbanks (`.fil`) or .fits file format. The raw voltages are recorded and then processed into usable Stoke I files.

2.3 Search Strategy

A zoo of pulsar software has been developed over the past decades to detect and time pulsars. One of the most commonly used softwares in the search for binary pulsars is PRESTO (Ransom, 2001). The search is carried out as illustrated in fig. 2.2 and due

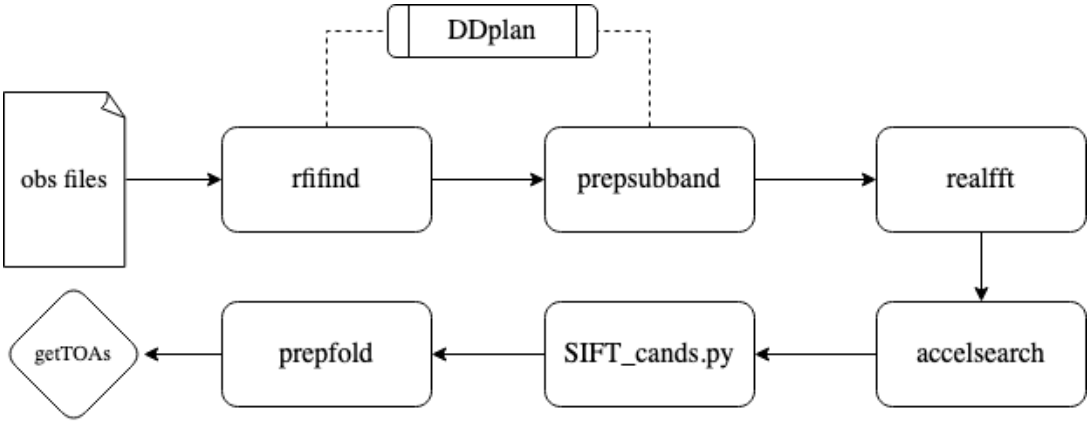

Figure 2.2: Outline of the PRESTO search strategy used to search for binary pulsars.

to the large data volumes produced by modern telescopes, the search is carried out in a distributed manner on high performance computing clusters.

2.3.1 RFI Removal

The first step in nearly all radio observations is to remove Radio Frequency Interference (RFI) from the observations data, this is usually caused by most modern technologies. This is important as artifical signals can mimic period signals associated with pulsar emission. Thus the data must mask frequencies or be clipped in the time domain. This project makes use of `rfifind` to remove such RFI.

`rfifind` which is part of the PRESTO suite searches in both frequency and time domains. It analyses each channel for a specified time integration. Firstly the time domain statitics are computed which consists of the mean and stadared deviation of the values in each channel. For blocks where the mean value exceeds 4σ the block is flagged as RFI. If more than 30% of the channel is flagged the entire channel is masked completely and replaced with a median constant bandpass value. An example of a mask produced by `rfifind` is shown in fig. 2.4.

2.3.2 Incoherent Dedispersion

Following the masking of all observation files the next step is to inchoherently dedisperse the data. This is done to remove the effects of dispersion caused by the interstellar medium as discussed in X. Failure to de-disperse data broadens potential pulse profiles and significantly reduces the signal to noise ratio. Figure 2.3 shows an example of pulse dispersion. Inchoherent dedispersion is carried out by splitting the data into subbands and then shifting the data in time to correct for the desipersion.

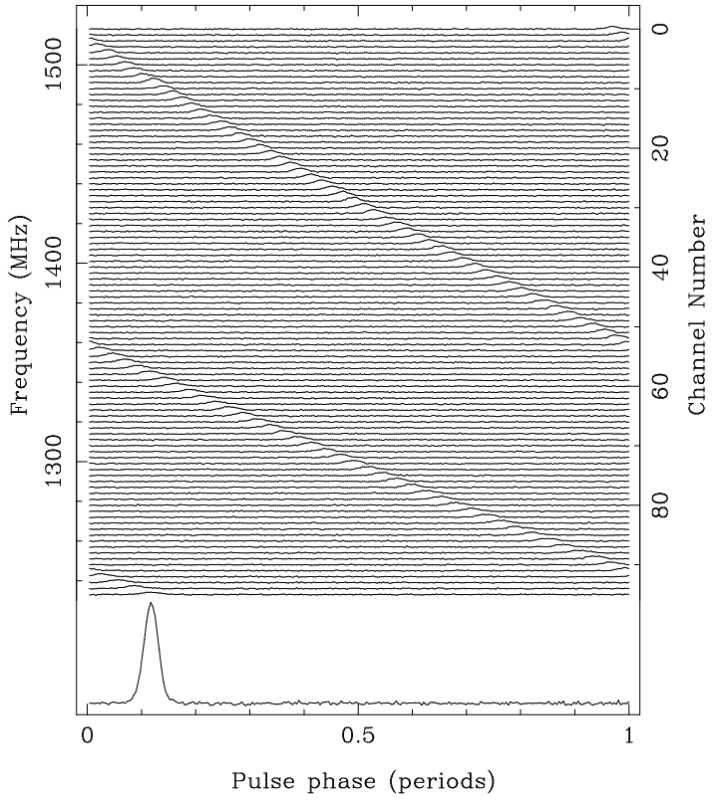

Figure 2.3: Example of a dispersion pulses of 128 ms pulsar B1356-60, which has a dispersion measure of 295 pc cm^{-3}. Figure from Lorimer and Kramer (2004, p. 20).

When correcting for dispersion it is important to consider the possible range of DMs that the pulsar could exhibit. The DM can be estimated through the use of density electron models such as X and X. However when dedisperseing the data it inherently induces smearing in the data. There are four types of smearing that need to be acounted for and characterized by the following equation,

$$\tau_{\text{total}} = \sqrt{\tau_{\text{samp}}^2 + \tau_{\text{sub}}^2 + \tau_{\text{BW}}^2 + \tau_{\text{chan}}^2} \tag{2.2}$$

2.3.3 Fast Fourier Transform

The data is needs to be transformed into the frequency domain to search for periodic signals. This is commonly done with a Discrete Fourier Transform (DFT) in pulsar astronomy and computationally carried out using a Fast Fourier Transform (FFT). For a time series, S_j of a given length of N it is neccessary to convert the time series into the barycentric frame of reference. The barycentric frame if reference point is centered on the mass of the solar system.
The kth Fourier component of the time series is described in Lorimer and Kramer (2004, pp. 132-134) as,

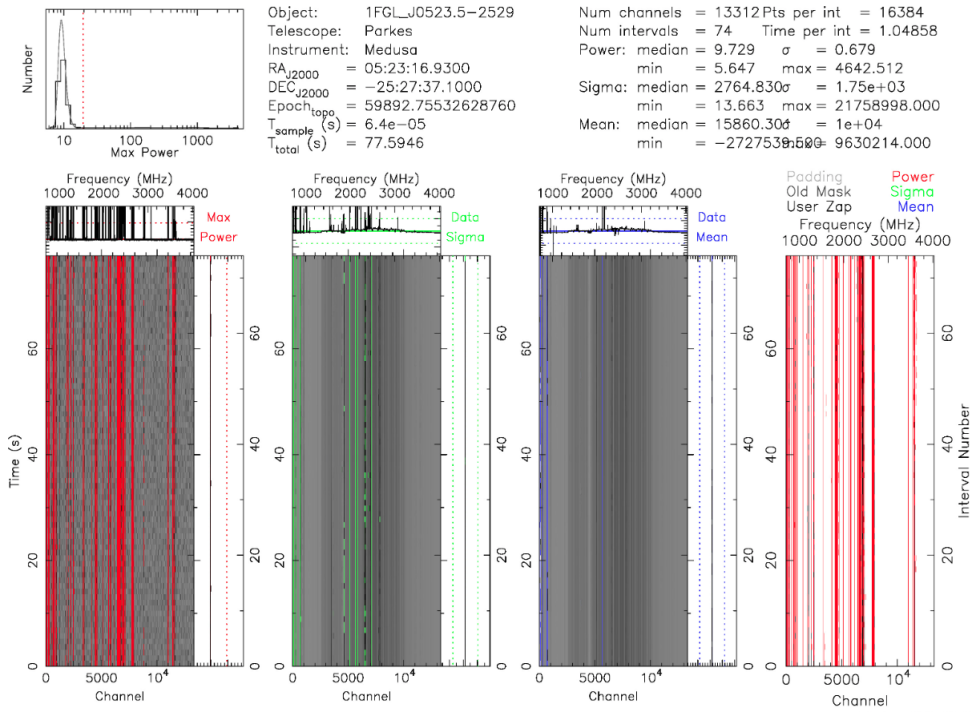

Figure 2.4: Example of RFI removal using `rfifind` on a 77 second observation of J0523. The upper left panels shows the max power profile of the RFI detected. The bottom most left panel show the max power, the second panel to the right shows the σ, the third panel shows the mean and the right most panel is the reccomended mask with all panels plotted.

$$\mathcal{F}_k = \sum_{j=0}^{N-1} S_j \exp\left(-2\pi\sqrt{-1}\frac{jk}{N}\right) \tag{2.3}$$

To complete this computation it requires N^2 floating point opearations. However, if a FFT operation is employed the number of operations is reduced to $N \log_2 N$ for a time series of length N. Since the time series data are real numbers symmetry can be exploited as the DFT is symmetric about the Nyquist frequency, $\nu_{\rm Nyq} = 1/(2t_{\rm samp})$. For any frequencies higher than the $\nu_{\rm Nyq}$ the complex conjucate is the same as the corresponding lower half of the frequency.

On the software side this is carried out with the `realfft` function in PRESTO. This result intakes the dedisperesed subbands and returns the power spectrum of the data. At this point the data is in a state to be searched for periodic signals.

2.3.4 Accelration Searching

Searching for binary pulsars requires a slightly different approach as the motion of the system causes the observed pulse frequency to smear across the Fourier bins (Cherry's paper), in turn this reduces the sensitivity of the search. A solution to this is to split up

the search into smaller time intervals and assume that the radial velocity is a constant on this time scale. This can be shown to be a good approximation for $P_b/10$.
The spin frequency, f_{spin} and the time of pulse emission, t_{pulse} the pulsar's phase can be expressed as, $\phi_p = f_{\text{spin}} t_{\text{pulse}}$. Morever, the pulse time can be expressed as the time of arrival from the pulsar, $d(t_0)$,

$$t_{\text{pulse}} = t_0 - \frac{d(t_0)}{c} \tag{2.4}$$

thus the phase can be expressed as,

$$\phi_p = f_{\text{spin}} \left[t_0 - \frac{d(t_0)}{c} \right] \tag{2.5}$$

$$= f_{\text{spin}} \left[t_0 - \frac{a \sin i}{c} \sin \left[\frac{2\pi(t - t_{\text{asc}})}{P_B} \right] \right] \tag{2.6}$$

where a is the semi-major axis, i is the inclination angle, t_{asc} is the time of ascending node and P_B is the orbital period. A Taylor expansion can be used to $\sin x$ around $x = a$ such that,

$$\sin(x) \simeq \sin(a) + \cos(a)(x - a) - \frac{\sin(a)}{2!}(x - a)^2 - \frac{\cos(a)}{3!}(x - a)^3 + \dots \tag{2.7}$$

Therefore the phase of the pulsar with a constant spin down rate can be expressed as,

$$\phi(t) = f^1 t_0 + \frac{\dot{f}}{2}(t - t_0)^2 + \frac{\ddot{f}}{6}(t - t_0)^3 + \dots \tag{2.8}$$

Matching co-effcients between the the full Taylor expansion and the phase expression for the pulsar gives the following relation, $\dot{f}/2 = f_{\text{spin}} \frac{a \sin i}{c} A$. Where A is represents all the terms in the expansion. The final simplified expression works out to be,

$$\dot{f} = f_{\text{spin}} \frac{4\pi^2 a \sin i}{c P_B^2} \sin \left[\frac{2\pi(t - t_{\text{asc}})}{P_B} \right] \tag{2.9}$$

Thus over a small enough time period spin-down is approximately constant.

$$\frac{k_2 P_B}{2\pi q} = a \sin i \tag{2.10}$$

Where k_2 is the radial velovity semi-amplitude, P_B is the orbital period and q is the mass ratio.

Searching is carried out using `accelsearch` which searches the FFT time series for period

emissions by summing the highest Fourier frequency derivative. The number of bins that this signal is smeared is given by the acceleration parameter (Ransom, 2001),

$$z \simeq \dot{f} T_{\mathrm{obs}}^2 \tag{2.11}$$

Where T_{obs} is the length of the observation. The search is carried out over a range of accelerations which can be based on eq. (2.10) if the physical quantities are known. A list of the known orbital parameters for the two candidates is given in table 1 along with resultant z values.

Candidate	P_{orb} (days)	k_2 (kms^{-1})	$a \sin i$ (s)	e	q	z
J0523.5-2529	0.68813	190.3	0.359	0.040	0.61 ± 0.06	
J2054						

Table 1: Orbital parameters of the two candidates. Values for J0523 are taken from Strader et al. (2014) and Halpern et al. (2022). Values for J2054 are taken from Karpova et al. (2023).

3 Summary

References

G. Baym, H. A. Bethe, and C. J. Pethick. Neutron star matter. *Nuclear Physics A*, 175 (2):225–271, Nov. 1971. ISSN 0375-9474. doi: 10.1016/0375-9474(71)90281-8. URL https://www.sciencedirect.com/science/article/pii/0375947471902818.

S. Chandrasekhar. *An Introduction to the Study of Stellar Structure*. Dover Books on Astronomy Series. Dover Publications, Incorporated, 1967. ISBN 978-0-486-13628-8. URL https://books.google.ie/books?id=joWn8s2BF04C.

J. P. Halpern, K. I. Perez, and S. Bogdanov. Luminous Optical and X-ray Flaring of the Putative Redback Millisecond Pulsar 1FGL J0523.5$-$2529. *The Astrophysical Journal*, 935(2):151, Aug. 2022. ISSN 0004-637X, 1538-4357. doi: 10.3847/1538-4357/ac8161. URL http://arxiv.org/abs/2207.08198. arXiv:2207.08198 [astro-ph].

A. Heger, C. L. Fryer, S. E. Woosley, N. Langer, and D. H. Hartmann. How Massive Single Stars End Their Life. *The Astrophysical Journal*, 591:288–300, July 2003. ISSN 0004-637X. doi: 10.1086/375341. URL https://ui.adsabs.harvard.edu/abs/2003ApJ...591..288H. ADS Bibcode: 2003ApJ...591..288H.

A. Hewish, S. J. Bell, J. D. H. Pilkington, P. F. Scott, and R. A. Collins. Observation of a Rapidly Pulsating Radio Source. *Nature*, 217(5130):709–713, Feb. 1968. ISSN 1476-4687. doi: 10.1038/217709a0. URL https://doi.org/10.1038/217709a0.

A. V. Karpova, D. A. Zyuzin, Y. A. Shibanov, and M. R. Gilfanov. A new redback pulsar candidate 4FGL J2054.2+6904. *Monthly Notices of the Royal Astronomical Society*, 524 (2):3020–3025, July 2023. ISSN 0035-8711, 1365-2966. doi: 10.1093/mnras/stad1992. URL http://arxiv.org/abs/2306.17593. arXiv:2306.17593 [astro-ph].

V. M. Kaspi, M. E. Roberts, G. Vasisht, E. V. Gotthelf, M. Pivovaroff, and N. Kawai. Chandra X-Ray Observations of G11.2-0.3: Implications for Pulsar Ages. *The Astrophysical Journal*, 560:371–377, Oct. 2001. ISSN 0004-637X. doi: 10.1086/322515. URL https://ui.adsabs.harvard.edu/abs/2001ApJ...560..371K. ADS Bibcode: 2001ApJ...560..371K.

J. M. Lattimer and M. Prakash. Neutron Star Structure and the Equation of State. *The Astrophysical Journal*, 550(1):426, Mar. 2001. ISSN 0004-637X. doi: 10.1086/319702. URL https://dx.doi.org/10.1086/319702.

D. R. Lorimer and M. Kramer. *Handbook of Pulsar Astronomy*, volume 4. Cambridge University Press, 2004.

F. C. Michel. Theory of pulsar magnetospheres. *Reviews of Modern Physics*, 54(1):1–66, Jan. 1982. doi: 10.1103/RevModPhys.54.1. URL https://link.aps.org/doi/10.1103/RevModPhys.54.1. Publisher: American Physical Society.

J. R. Oppenheimer and G. M. Volkoff. On Massive Neutron Cores. *Physical Review*, 55 (4):374–381, Feb. 1939. doi: 10.1103/PhysRev.55.374. URL https://link.aps.org/doi/10.1103/PhysRev.55.374. Publisher: American Physical Society.

S. M. Ransom. *New search techniques for binary pulsars*. PhD thesis, Jan. 2001. URL https://ui.adsabs.harvard.edu/abs/2001PhDT.....123R. Publication Title: Ph.D. Thesis ADS Bibcode: 2001PhDT.....123R.

P. S. Ray, A. A. Abdo, D. Parent, D. Bhattacharya, B. Bhattacharyya, F. Camilo, I. Cognard, G. Theureau, E. C. Ferrara, A. K. Harding, D. J. Thompson, P. C. C. Freire, L. Guillemot, Y. Gupta, J. Roy, J. W. T. Hessels, S. Johnston, M. Keith, R. Shannon, M. Kerr, P. F. Michelson, R. W. Romani, M. Kramer, M. A. McLaughlin, S. M. Ransom, M. S. E. Roberts, P. M. S. Parkinson, M. Ziegler, D. A. Smith, B. W. Stappers, P. Weltevrede, and K. S. Wood. Radio Searches of Fermi LAT Sources and Blind Search Pulsars: The Fermi Pulsar Search Consortium, May 2012. URL http://arxiv.org/abs/1205.3089. arXiv:1205.3089 [astro-ph].

R. W. Romani, D. Kandel, A. V. Filippenko, T. G. Brink, and W. Zheng. Psr j0952-0607: The fastest and heaviest known galactic neutron star. *The Astrophysical Journal Letters*, 934(2):L17, jul 2022. doi: 10.3847/2041-8213/ac8007. URL https://dx.doi.org/10.3847/2041-8213/ac8007.

J. Strader, L. Chomiuk, E. Sonbas, K. Sokolovsky, D. J. Sand, A. S. Moskvitin, and C. C. Cheung. 1FGL J0523.5-2529: A New Probable Gamma-ray Pulsar Binary. *The Astrophysical Journal*, 788(2):L27, June 2014. ISSN 2041-8205, 2041-8213. doi: 10.1088/2041-8205/788/2/L27. URL http://arxiv.org/abs/1405.5533. arXiv:1405.5533 [astro-ph].

J. Takata, K. L. Li, G. C. K. Leung, A. K. H. Kong, P. H. T. Tam, C. Y. Hui, E. M. H. Wu, Y. Xing, Y. Cao, S. Tang, Z. Wang, and K. S. Cheng. Multi-wavelength emissions from the millisecond pulsar binary psr j1023+0038 during an accretion active state. *The Astrophysical Journal*, 785(2):131, Apr. 2014. ISSN 0004-637X. doi: 10.1088/0004-637X/785/2/131. URL https://dx.doi.org/10.1088/0004-637X/785/2/131. Publisher: The American Astronomical Society.

J. H. Taylor and R. N. Manchester. Recent observations of pulsars. *Annual Review of Astronomy and Astrophysics*, 15:19–44, Jan. 1977. ISSN 0066-4146. doi: 10.1146/annurev.aa.15.090177.000315. URL https://ui.adsabs.harvard.edu/abs/1977ARA&A..15...19T. ADS Bibcode: 1977ARA&A..15...19T.